Investigating the effect of basalt fiber additive on the performance of clay barriers for radioactive waste disposals

Hajar Share Isfahani & Amin Azhari

Bulletin of Engineering Geology and the Environment
The official journal of the IAEG

ISSN 1435-9529

Bull Eng Geol Environ
DOI 10.1007/s10064-020-02044-x

Springer

Bulletin of Engineering Geology and the Environment
https://doi.org/10.1007/s10064-020-02044-x

ORIGINAL PAPER

Investigating the effect of basalt fiber additive on the performance of clay barriers for radioactive waste disposals

Hajar Share Isfahani[1] · Amin Azhari[2]

Received: 28 December 2019 / Accepted: 6 November 2020

Abstract

Radioactive materials are widely used in mining, manufacturing, medicine, and agricultural processes. The waste products from these materials are hazardous and should be appropriately dumped. As a result, a proper radiation shielding barrier is required to avoid the contamination of the surrounding environment. Clay soil is an efficient and eco-friendly radiation shielding material, which is commonly used to cap the hazardous and radioactive landfills. In this research, the effects of basalt fiber additive in four percentages, including 0.5, 1, 2, and 5 on the bentonite clay radiation shielding performance, were investigated using experimental and simulation methods. Also, the permeability of the mixtures is controlled to be in the acceptable range as a vital parameter for radioactive disposal barriers. Chemical and microstructure analyses were conducted on the utilized material, using energy-dispersive X-ray spectroscopy (EDX) and scanning electron microscopy (SEM). Linear attenuation coefficient (μ), representing the material radiation shielding performance, was evaluated using the HPGe spectrometer detector, MCNP simulation code, and XCOM web program on the three commonly used gamma-ray energy levels of ^{137}Cs (661.6 keV) and ^{60}Co (1173.5 and 1332.5 keV). An acceptable agreement was observed between experimental and simulation results, revealing that adding basalt fiber improves the shielding performance due to a higher linear attenuation coefficient (μ), where 2% of basalt fiber leads to the highest values of 12.3 m^{-1}, 10.14 m^{-1}, and 8.5 m^{-1} obtained for 661.6 keV, 1173.2 keV, and 1332.5 keV energy levels, respectively. The results concluded that, due to radiation shielding performance, workability, and permeability limitations, the 2% basalt-bentonite mixture could be a new candidate covering low-level radioactive waste disposal.

Keywords Bentonite clay · Basalt fiber · Radiation shielding · Radioactive waste management · Permeability

Introduction

The management of radioactive waste is a great environmental concern in industrial countries. Public concerns about low-level radioactive waste (LLRW) disposal sites have been addressed in different environmental perspectives. It is inevitable to consider a cover layer to surround and cap the LLRW disposals, to prevent the contamination of soil and groundwater sources around these disposals. Generally, two main factors control selecting a suitable LLRW cover layer, fluid permeability, and radiation shielding characteristics (Barron and Dickman 1949; Auerbach 1958; Murphy et al. 1989; Ryan 1998; Weisstein 2003; Hicks et al. 2008; and Shultis and Faw 2012).

Generally, high-density materials, such as lead, magnetite, high-density grout, barite, and polyethylene plastic, are known as material attenuating the radiation exposure from radioactive sources. Basalt fiber as a high-density material has been widely used as an additive in various materials attenuating the gamma-ray radiation, including concrete, building material, polymer, resin, and epoxy composites (Hou et al. 2018; Li et al. 2017a; Li et al. 2017b; Mahmoud et al. 2019; Medjahed et al. 2019; Romanenko et al. 2019; Skarżyński 2020; Zegaoui et al. 2019; Zegaoui et al. 2020; Zorla et al. 2017). Romanenko et al. (2019) investigated the effect of basalt-boron fiber additives with different dosages on radiation shielding performance of concrete used in waste management applications. They have shown a remarkable increase of

✉ Hajar Share Isfahani
hajarshare@iut.ac.ir

Amin Azhari
aazhari@iut.ac.ir

[1] Department of Civil Engineering, Isfahan University of Technology, Isfahan 84156-83111, Iran

[2] Department of Mining Engineering, Isfahan University of Technology, Isfahan 84156-83111, Iran

Published online: 19 November 2020

up to 13% for neutron radiation shielding properties of high concentrations of basalt-baron fiber in concrete. A study is performed on the radiation shielding and mechanical property improvement of a novel basalt fiber/phthalonitrile composite compared to the monolithic alloy. The results showed an effective gamma-ray shielding performance enhancement of 25 to 43% depending on the composite thickness. Li et al. (2017c) conducted a study on the radiation shielding performance of a structural polymer composite against the gamma-ray, using basalt fiber-reinforced epoxy as additive. The experimental and theoretical (XCOM database) results showed a drastic decrease of up to 63% in photon intensities. Another study examined the radiation shielding improvement of epoxy matrix composites using basalt fibers as additives. They used 5.9 to 33.1 wt% of this additive. The experimental and theoretical results show an acceptable agreement with mass attenuation coefficient increment of up to 2.1 (cm^2/g) for the highest amount of additive compared to the raw resin (Hu et al. 2008). Zegaoui et al. (2019) explored the effect of hybrid basalt/glass fibers on gamma radiation shielding properties of DCBA/BA resin composite. Their results show an average of 0.129 cm^{-1} for 30 wt% short basalt fibers. The desired half-value length (HVL) and tenth-value length (TVL) of the mixture notably reached the lowest point at 5.02 cm and 16.68 cm.

This characteristic of high-density material swayed engineers toward using these materials as additives to LLRW liners. In particular, hydraulic permeability is a controlling parameter in LLRW disposal design in addition to radiation shielding. Therefore, clay as a low hydraulic permeability material is commonly used in the lining structure of these constructions. Clay-based liners modified with high-density additives, as natural, cost-effective, and eco-friendly have been recently used as protective material covering these disposals (Divya et al. 2017b, 2017a; Isfahani et al. 2019a; Li et al. 2017a; Ono et al. 2018; Prakash and Poulose 2016; Isfahani et al. 2019b). The gamma-ray shielding and water permeability of barite powder-bentonite clay mixture were investigated as the cover layer in radioactive waste disposal. The result indicated that the mixture has an effective performance in radiation shielding, insofar as clay mixture with 40% barite powder would overcome concrete regarding gamma-ray shielding performance (Isfahani et al. 2019b). Also, steel slag as the by-product of steel factories has been applied as an additive to bentonite clay to improve the clay radiation shielding performance. The gamma-ray shielding performance of clay mixed with different percentages of steel slag was evaluated using both experimental and simulation methods at the three energy levels of 661.6, 1173.2, and 1332.5 keV. The results showed that adding steel slag to bentonite clay has a significant effect on the radiation shielding performance and the bentonite clay-steel slag mixture was represented as a respectable choice for radiation shielding material (Isfahani et al. 2019a). The photon energy absorption parameters for five different soil samples were examined (Kucuk et al. 2012). This research was performed using experimental measurement with ^{137}Cs and ^{60}Co as radioactive point gamma sources. According to their findings, clay loam and clay soils demonstrated suitable photon energy absorption performance. Mann et al. (2016b) investigated the burnt clay bricks as a radiation shield for storage disposal of radioactive waste material in the energy range of 0.001–15 MeV. The results revealed that clay bricks are suitable and environmentally safe candidates for radiation shielding barriers used in low-level radioactive waste disposal. Another research evaluated the radiation shielding performance of different mixtures including clay-white cement, clay-silica fume, gypsum, gypsum-silica fume, cement, white cement, cement-silica fume, white cement-gypsum, white cement-silica fume, red mud-silica fume, silica fume, and red mud at different energy levels (Akbulut et al. 2015). The results showed that clay, especially clay-white cement mixture, has the best performance in radioactive shielding among the investigated samples. Mann et al. (2016a) studied the effect of novel lightweight clay-fly ash bricks at gamma-ray shielding using the experimental method at four levels of gamma-ray energies, including ^{241}Am (59.4 keV), ^{137}Cs (661.6 keV), and ^{60}Co (1173.2 keV and 1332.5 keV). The results showed that these bricks could effectively attenuate the moderate energy of gamma-ray and can be used for building construction where radiation shielding is required.

Authors' previous studies mainly focused on improving the radiation shielding performance of clay bentonite liner of landfills using steel slag and barite powder as high-density additives. However, literature shows that using basalt fibers as an additive would be able to improve the radiation shielding performance of construction material, mostly concrete. Therefore, the present study aimed at investigating the effect of basalt fiber additives to clay soil on the performance of clay as the base material for the LLRW disposal liners, which has not been studied earlier. Regarding the fact that radiation shielding and hydraulic permeability are the two main factors for the LLRW liners, in this study, these two governing factors are evaluated on the modified bentonite clay employing various dosages of the basalt fiber additive.

Materials and methods

Materials

Bentonite clay as the base material and basalt fibers as an additive are used in this research. Bentonite clay consists more than 95% montmorillonite minerals and relatively impermeable soils usually used in landfill cover layers (Seed et al. 1964; Day et al. 1999; and Koch 2002). The utilized bentonite in this research is a calcium-base bentonite with the grading curve

illustrated in Fig. 1. The figure shows that the grain sizes are generally less than 0.075 mm and mainly between 0.00045–0.001 mm and 0.003–0.075 mm. Moreover, the specific gravity, the permeability coefficient, and the Atterberg's limits, including plastic limit (PL) and liquid limit (LL), were obtained according to the ASTM Standard D 4318, presented in Table 1.

Basalt fibers, made from particularly fine fibers of basalt with high performance and low-cost, are considered to improve the bentonite clay radiation shielding. Chemical and physical properties of the basalt fibers are presented in Table 2.

Chemical and microstructural analyses for the bentonite clay (BC) and the basalt fibers (BF) were conducted using EDX and SEM. The chemical compositions and SEM images for the employed materials are presented in Table 3 and Fig. 2, respectively. The obtained results are employed for the following theoretical analyses and simulations.

Sample preparation

The mixture of the bentonite clay with different percentages of the basalt fiber including, 0.5%, 1%, 2%, and 5% are prepared. It should be noted that adding fibers of more than 2% is not usual, due to creating issues such as complicated mixing process, low workability, and high inhomogeneity (Hejazi et al. 2012). However, in this research, a sample with 5% basalt fiber is also examined as a controlling point for the effect of higher additive percentages on the bentonite shielding performance.

After mixing the bentonite clay with considered percentages of basal fiber, the optimum moisture content and the corresponding density of each mixture is obtained from the proctor compaction test, according to ASTM D698. In the compaction test, the mixtures are compacted in a cylindrical mold with 101.6-mm diameter and 116.43-mm height with 2.5-kg rammer dropped from a height of 305 mm, to

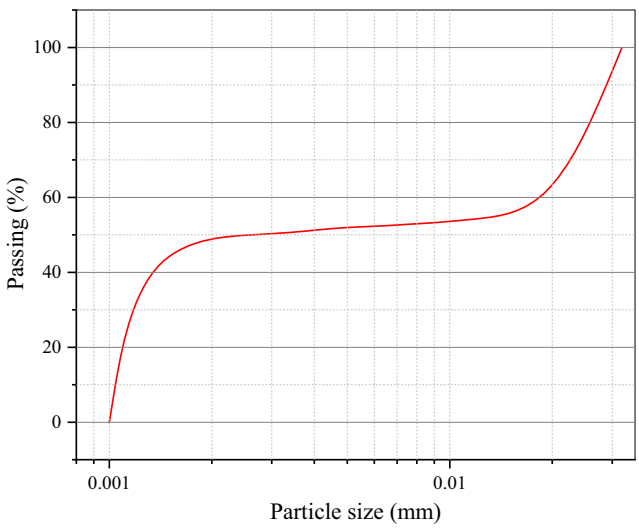

Fig. 1 The particle grading curve of utilized bentonite

Table 1 The four significant technical properties of utilized bentonite

Parameters	Value	Standard
Density (g/cm^3)	1.6	–
Specific gravity	2.34	ASTM D854
Liquid limit (LL)%	120	ASTM D 4318-93
Plastic limit (PL)%	32	ASTM D 4318-93
Coefficient of permeability (cm/s)	7.8×10^{-9}	ASTM D 5856-95

determine the relationship between water content and dry unit weight of the mixture. Optimum moisture content (w_{opt}) and maximum dry unit weight values of the samples are then determined. The specifications of each mixture are presented in Table 4.

Two sets of tests are performed for this study, defining radiation shielding performance and hydraulic permeability of the mixtures. The following describes the sample preparation procedure for the tests.

Three cylindrical samples with 5-cm diameter and 2-, 4-, and 6-cm thickness are prepared to define the radiation attenuation coefficient (μ) using the HPGe detector for each mixture. The three samples are prepared in the desired moisture content and the corresponding density (presented in Table 4). Considering the volume of the test mold and the desired density, the required weight of the mixture is placed in the test mold and compacted to fill the molds with heights of 2, 4, and 6 cm.

For the hydraulic permeability tests, water is added to the mixture to reach the optimum moisture content. The sample is formed in a cylindrical cell with a 10-cm diameter and 11-cm height. In the preparation procedure, the mixture is poured into the mold in three layers, and each layer is compacted by 25 drops of the 2.5-kg standard hammer.

Experimental radiation shielding test

In the used experimental setup shown in Fig. 3, a narrow beam of radiation is applied to the sample, and the intensity of the transferred radiation is measured by a high-purity germanium detector (HPGe). The ^{137}Cs (661.6 keV) and ^{60}Co (1173.2 and 1332.5 keV) are employed as the radiation sources to apply the three commonly used energy levels. Two steel collimators

Table 2 The chemical and physical properties of the used basalt fiber

Properties	Value	Standard
Density (g/cm^3)	2.67	
Tensile strength (MPa)	3000	ASTM C1557
Modulus of elasticity (GPa)	79	ASTM C1557
Diameter (μm)	17	_

Table 3 Chemical analysis of BC and BF

Element	BC	BF
O	42.8	61.1
Al	8.39	7.6
Si	41.51	15.5
Ca	3.55	–
Fe	3.75	–
Mg	–	5.9
Na	–	10

are utilized on the top and bottom of the sample, to reach the proper narrowness of the irradiation geometry (Fig. 3). The HPGe records the radiation intensity with and without samples, noted as I and I_0, respectively.

The Beer-Lambert law describes the radiation attenuation in shielding materials. According to this law, the attenuation coefficient (μ) for each shielding material is calculated using Eq. 1 (Chilton et al. 1984; Krane and Halliday 1988; Martin 2006).

$$I = I_0 e^{-\int_0^t \mu \, dx} \tag{1}$$

where I and I_0 are gamma-ray intensity with and without barrier, respectively, and t is the thickness of the barrier. For homogeneous and isotropic shielding material, the equation can be modified in the following form:

$$I = I_0 e^{-\mu t} \tag{2}$$

Considering Eq. 2, the uncertainty of μ in experimental measuring can be estimated using the error propagation formula:

$$\Delta(\mu) = \frac{1}{t}\sqrt{\left(ln\left(\frac{I_0}{I}\right)\right)^2\left(\frac{\Delta t}{t}\right)^2 + \left(\frac{\Delta I_0}{I_0}\right)^2 + \left(\frac{\Delta I}{I}\right)^2} \tag{3}$$

where, ΔI_0, ΔI, and Δt are experimental errors for I_0, I, and t values, respectively.

The half-value layer (HVL) and tenth-value layer (TVL) are the required thicknesses of the radiation shielding material to decrease the intensity of the gamma-ray to 50 and 10%, respectively. According to the definition, HVL and TVL are calculated using the bellow equations (Jaeger et al. 1968):

$$\mathrm{HVL} = \frac{Ln(2)}{\mu}\ (\mathrm{m}) \tag{4}$$

$$\mathrm{TVL} = \frac{Ln(10)}{\mu}\ (\mathrm{m}) \tag{5}$$

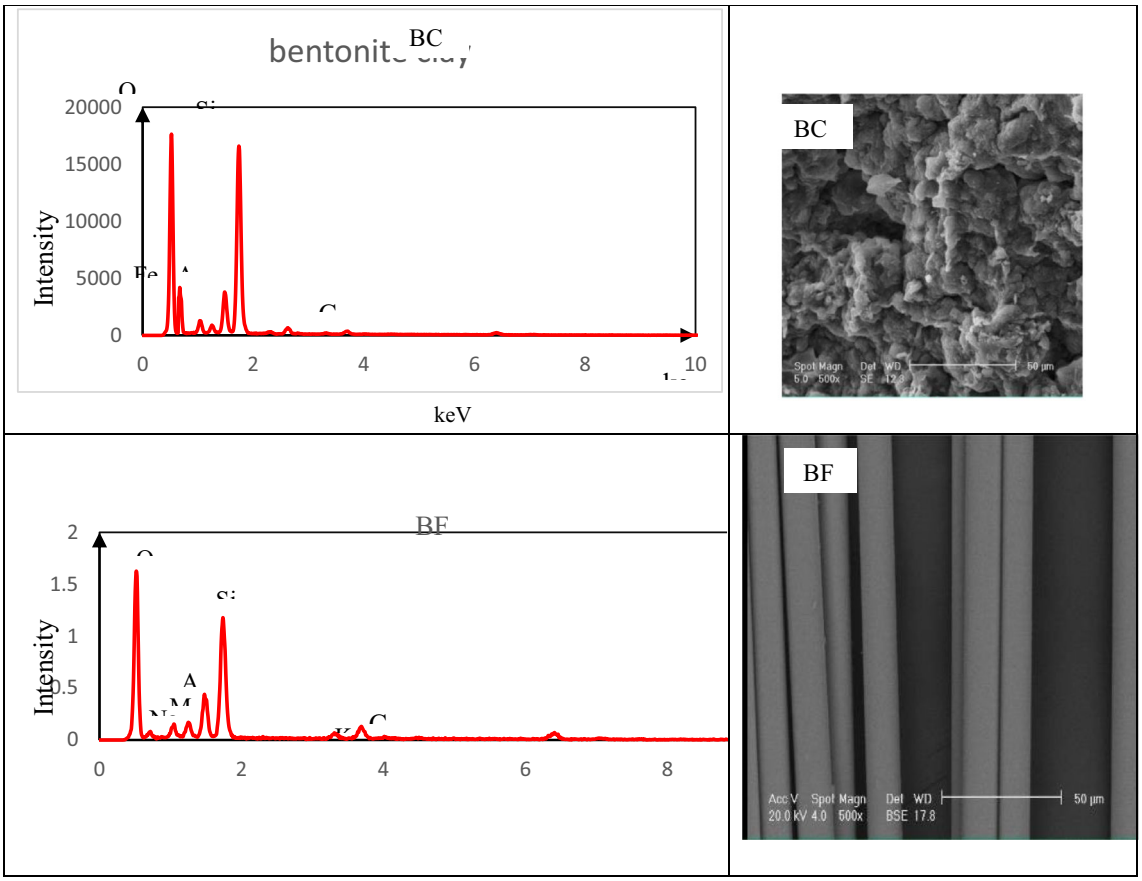

Fig. 2 EDX graphs and SEM images for BC and BF

Table 4 Specifications of investigated mixtures

Materials	Percentage in mixture %	Sample code	w_{opt}	Maximum dry density
Bentonite clay	100	BC	28	1.24
Bentonite clay-basalt fiber	99.5–0.5	BCBF1	31	1.18
Bentonite clay-basalt fiber	99–1	BCBF2	32	1.21
Bentonite clay-basalt fiber	98–2	BCBF3	42.5	1.13
Bentonite clay-basalt fiber	95–5	BCBF4	34	1.14

The attenuation coefficient, half-value layer (HVL), and tenth-value layer (TVL) are then calculated from the measures radiation intensities (I and I_0) and above equations.

Radiation shielding simulation (MCNP)

In this study, the radiation shielding procedure for the intended materials was simulated using the Monte Carlo N-Particle Transport Code (MCNP) and evaluated using the XCOM web base program (Briesmeister 2000). The Monte Carlo method is a wide-ranging class of computational algorithms that are based on a repeated random sampling to find numerical results (Kroese et al. 2014). For simulating the radiation shielding in MCNP code, cells are defined for each material and the material properties are assigned considering their atomic number and atomic mass number according to Eq. 6. The 2D and 3D images of the generated cells including the sample, free space (air), and the steel collimators arranged according to the experimental setup are shown in Fig. 4.

$$\mathrm{ZAID} = Z \times 1000 + A \tag{4}$$

where ZAID is the assigned value to each cell, Z is the atomic number, and A is the atomic mass number.

After defining the cells and assigning the material and the radiation source energy levels used in the experimental tests, a cluster of rays is shot toward the sample, and different states that may occur, such as absorption, attenuation, and scattering, are randomly detected. This procedure is conducted with and without a sample to obtain the gamma-ray intensities I and I_0, respectively. Then, the linear attenuation coefficient (μ) is calculated using the Beer-Lambert law (Eq. 2).

Theoretical calculation of radiation shielding (XCOM)

The XCOM is used to estimate the photon cross sections for scattering, photoelectric absorption, pair production, and total attenuation coefficients for elements, compounds, and mixtures at different energies from 1 keV to 100 GeV. The total attenuation coefficients for mixtures and compounds are driven as the summation of the corresponding atomic constituent's quantities. Then, the weighting factors defined as the fractions by weight of the constituents are calculated by XCOM from the chemical formula. However, considering the mixtures, the

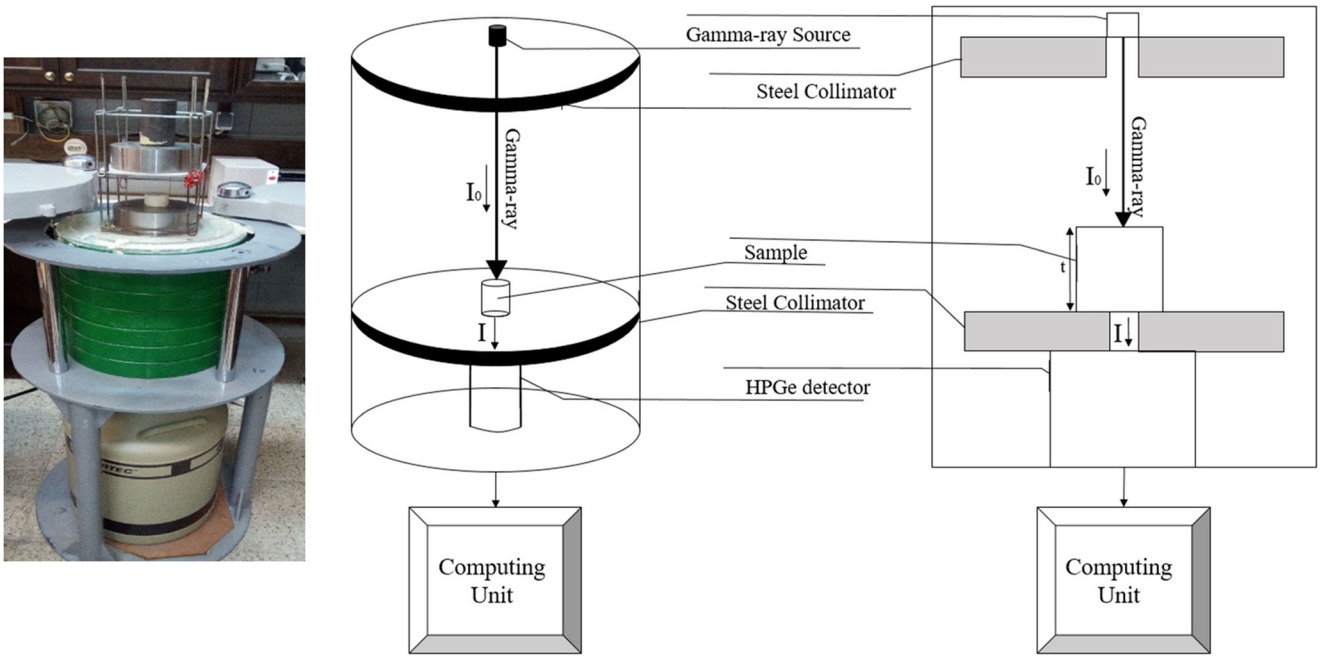

Fig. 3 Schematic view of the experimental radiation shielding test setup

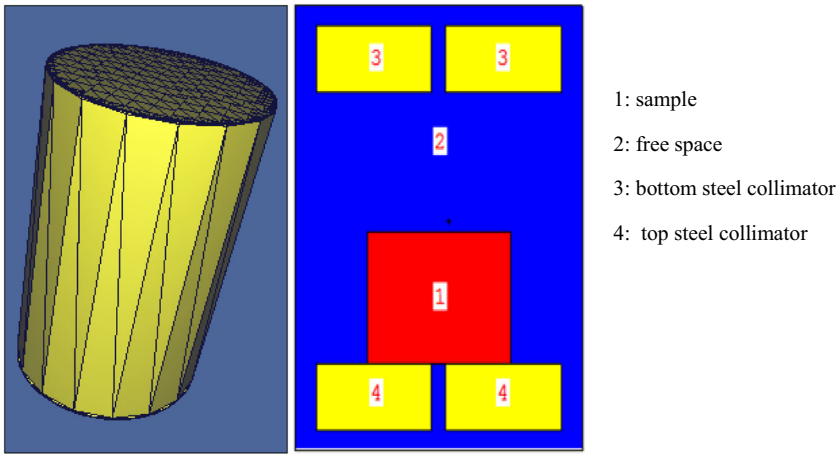

Fig. 4 2D and 3D images of simulated models using MCNP

fractions by weight of the components should be defined by the user (NIST XCOM 2010). In this research, the linear attenuation coefficient (μ) for the intended materials is calculated at three energy levels of 661.6, 1173.2, and 1332.5 keV.

Permeability measurement

As noted, the permeability of the clay liner should be less than 1×10^{-7} cm/s based on the EPA standard. As a result, the permeability test is conducted on all five mixtures to evaluate the effect of basalt additive. The test has been done, according to ASTM D5856-95. Due to the very low permeability of the mixture, a water head of 300 kPa is implemented in the test. The discharge volume rate is measured until it reaches a constant value. Then, the permeability (k) is calculated using the equation below:

$$k = \frac{Ql}{Aht} \tag{6}$$

where Q is the discharge volume (m^3), l is the specimen length (m), A is the specimen area (m^2), h is the water head (m), and t is time (s).

Results and discussion

From the literature, the density is directly related to the linear attenuation coefficient, and with attention to the basalt fiber density, it is expected that the higher basalt fiber dosages may lead to higher mixture density due to its significantly higher density compared to the bentonite clay. On the other hand, adding basalt fiber creates micro-gaps in the bentonite structure, which may decrease the density. The interaction of these two effects controls the density of the mixtures. Figure 5 illustrates the SEM images of bentonite clay (BC) and two-percent basalt fiber bentonite clay (BCBF3). The image shows the uniform distribution of basalt fiber with random orientations. The created micro-gaps can also be observed in the BCBF3 SEM image, which could be estimated up to 100 μm in width. According to Fig. 6, by adding basalt fiber to the bentonite clay, a density drop is observed in BCBF1, which could be due to the created micro-gaps; while adding higher dosages of basalt fiber, the density increases in BCBF 2 and BCBF3. However, conversion is observed for 5% of the basalt fiber (BCBF4), which shows the predominant effect of micro-gap generation compared to the basalt fiber density in higher additive dosages.

The radiation permittivity (I) for each fiber-modified mixture is measured experimentally for samples with 2, 4, and 6 heights. The I_0 value is also obtained from performing the same test without the sample in energy levels of 661.6, 11.73.2, and 1332.5 keV, using ^{60}Co and ^{137}Cs sources.

The results from the radiation shielding test for the mixtures are presented in Figs. 7, 8, 9, where the $ln\left(\frac{I_0}{I}\right)$ values are plotted against the sample thickness (t) in the three energy levels. Based on the Beer-Lambert law (Eq. 1), it is expected to observe a linear relation between $ln\left(\frac{I_0}{I}\right)$ and sample thickness (t), where the line slope would be the linear attenuation coefficient (μ). The graphs show that with an acceptable approximation, a line could be fit on the values of each mixture, where the high linear correlation coefficient ($R^2 > 0.99$) verifies the accuracy of the test results for each mixture. Moreover, it is observed from these figures that the BCBF3 has the highest elevation. This can be explained by the fact that the sample with a higher linear attenuation coefficient (μ) would experience lower gamma-ray intensity (I). Regarding the fact that the I_0 value stays constant in a specific energy level, the $ln\left(\frac{I_0}{I}\right)$ value leads to the maximum value for BCBF3. The MCNP code and the XCOM database results are also compared and verified with the experimental results. The linear attenuation coefficient (μ) values for each mixture are reported in Table 5, along with the MCNP and XCOM outputs. In addition, the maximum experimental uncertainty calculated using Eq. 4 is also shown in the table. As seen, the

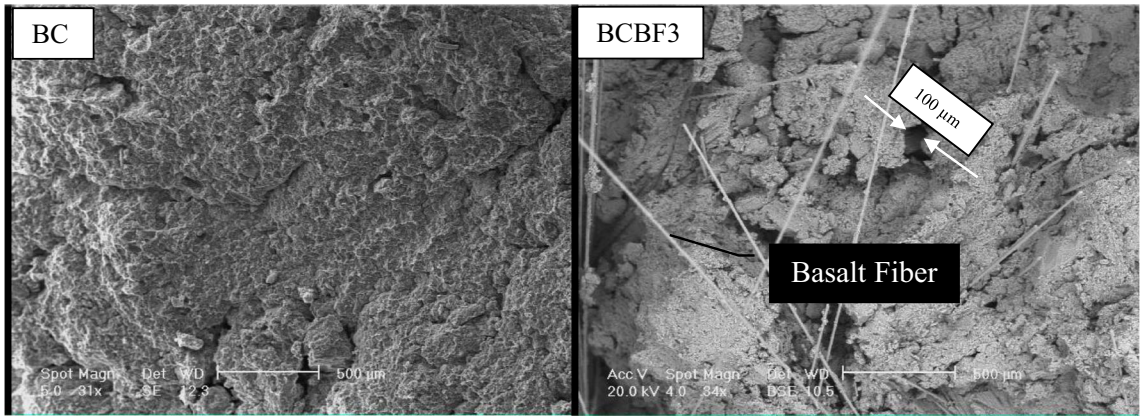

Fig. 5 SEM images for BC and BCBF3

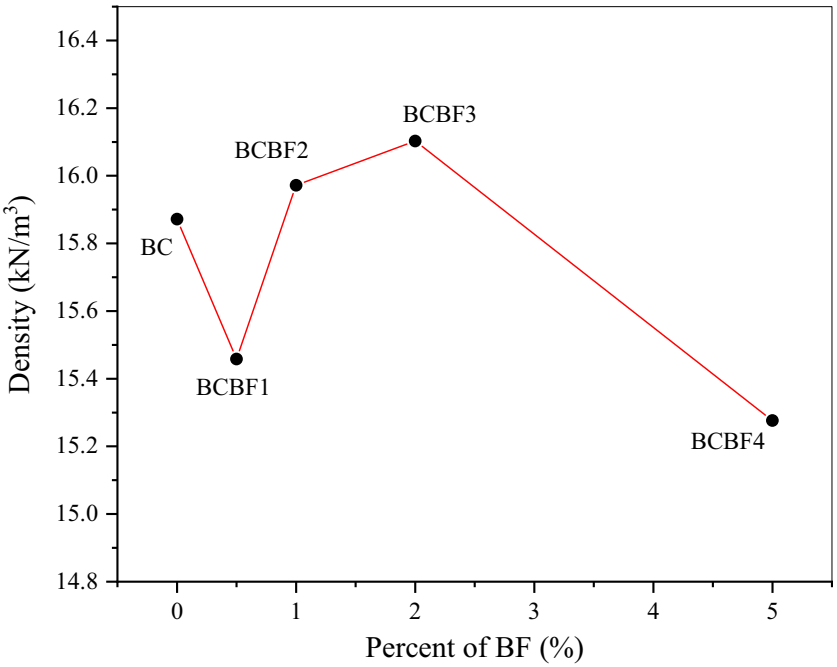

Fig. 6 The samples density values vs. the percent of basalt fiber

Table 5 The experimental and simulation results for linear attenuation coefficients (μ)

Factor	μ (1/m)											
	661.6 (keV)				1173.2 (keV)				1332.5 (keV)			
Mixture	Experimental		MCNP	XCOM	Experimental		MCNP	XCOM	Experimental		MCNP	XCOM
	μ	Δ(μ)			μ	Δ(μ)			μ	Δ(μ)		
BC	12.01	0.408	12.18	12.23	9.3	0.244	9.25	9.3	7.85	0.55	8.34	8.4
BCBF1	11.77	0.348	11.88	11.93	9.26	0.245	9.02	9.07	8.2	0.306	8.46	8.5
BCBF2	12.26	0.351	12.27	12.31	9.51	0.214	9.32	9.36	8.84	0.203	8.73	8.77
BCBF3	12.3	0.83	12.34	12.39	10.14	0.78	9.37	9.42	8.5	0.74	8.81	8.83
BCBF4	11.95	0.363	11.89	11.88	9.35	0.39	9.02	9.05	8.52	0.212	8.45	8.48

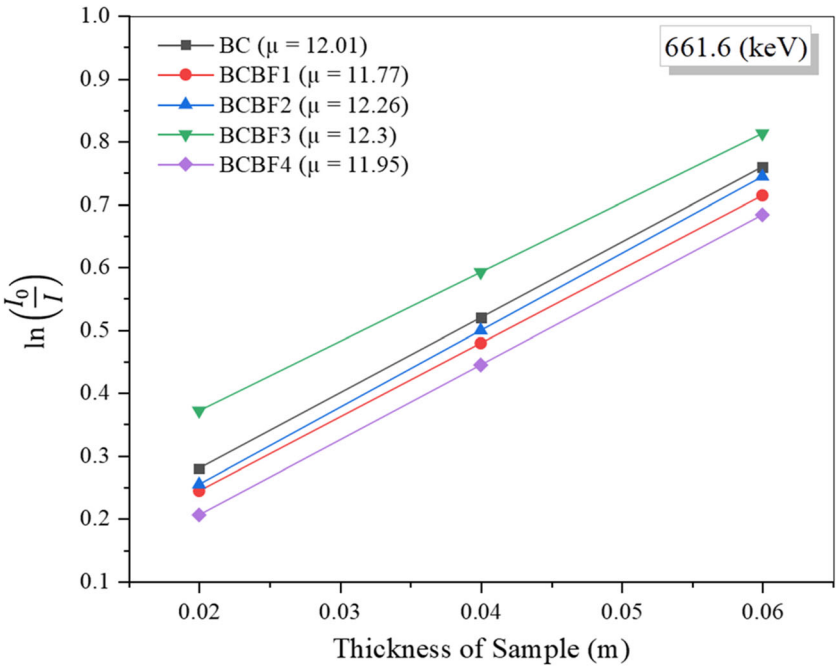

Fig. 7 The $\ln\left(\frac{I_0}{I}\right)$ vs. thickness trend from the experimental test at 661.6 keV

obtained values from the linear attenuation coefficient from MCNP code and XCOM are in good agreement with the experimental results.

Briefly, to better understand the effect of adding basalt fibers on the radiation shielding performance, the linear attenuation coefficient (μ) values vs. the percentage of the employed additive are plotted at these three levels of energy in Figure 10. As seen in this figure, for all considered cases, the linear attenuation coefficient (μ) is generally improved by increasing the percentage of the basalt fibers, up to 2%, and the maximum values are observed in BCBF3. However, the linear attenuation coefficient decreases at 5% of basalt fiber (BCBF4), compared to the BCBF3. The figure also reveals that linear attenuation coefficient (μ) values mimic the density (ρ) trend, which clearly shows the compatibility of the obtained experimental results, according to the following basic physics radiation shielding theory.

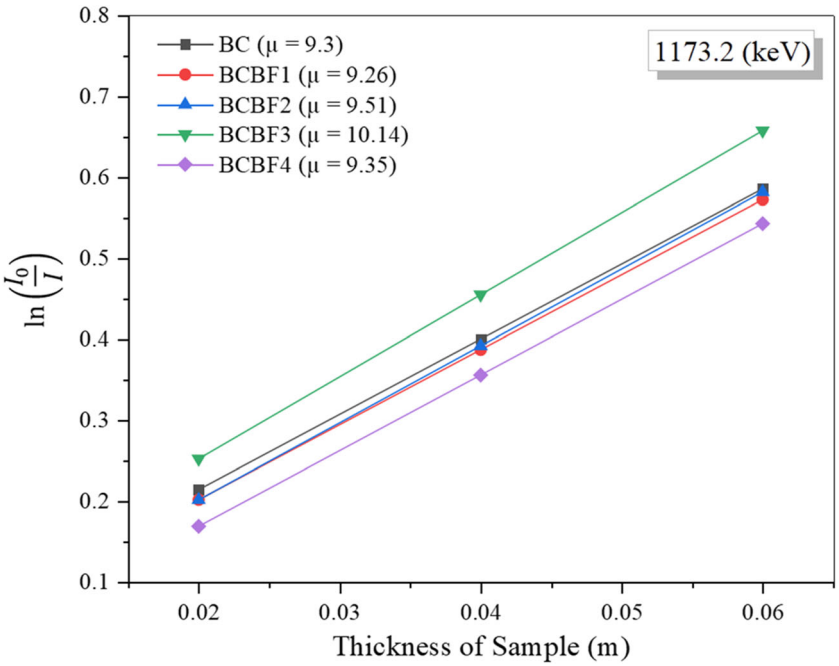

Fig. 8 The $\ln\left(\frac{I_0}{I}\right)$ vs. thickness trend from the experimental test at 1173.5 keV

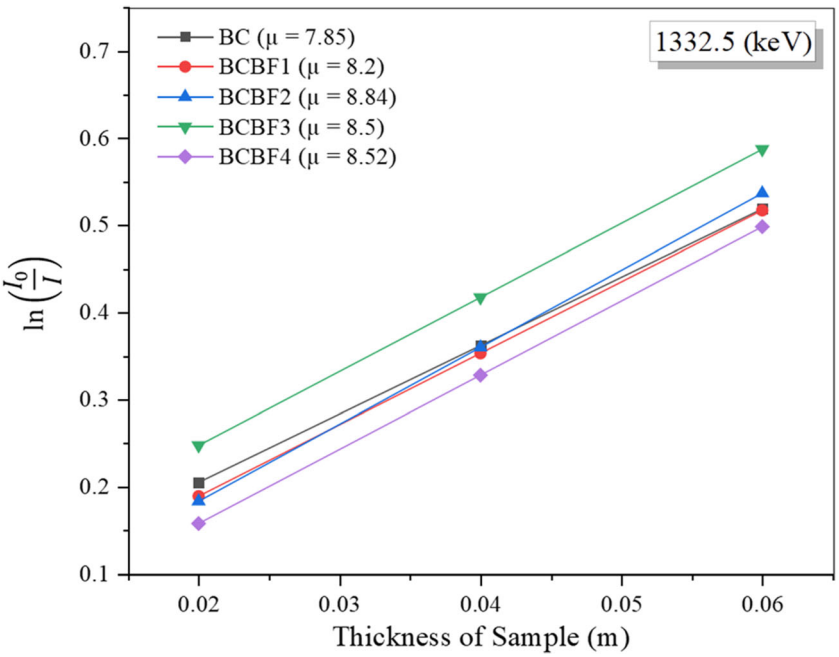

Fig. 9 The $\ln\left(\frac{I_0}{I}\right)$ vs. thickness trend from the experimental test at 1332.5 keV

The theory of radiation shielding designates that in the range of gamma-ray energies considered in this study (from $E_\gamma = 661.6$ keV for ^{137}Cs to $E_\gamma = 1332.5$ keV for ^{60}Co), the Compton scattering is the dominant interaction of photons with electrons. The Compton scattering is proportional to the $\frac{Z}{A}$ value (where Z is atomic, and A is the mass number) of the material, while $\mu \sim \frac{\rho Z}{A}$ (ρ is the density). The $\frac{Z}{A}$ values for all the used additive materials do not vary significantly. Therefore, it is expected that μ varies mainly with the density of the shielding material (Krane and Halliday 1988).

As mentioned in the theory of radiation shielding, HVL and TVL are parameters determining the required thickness of shielding materials. The calculated HVL and TVL values are presented in Table 6. The comparison of the HVL and TVL values of bentonite clay against basalt fiber clay samples indicates that using modified clay with up to 2% of basalt fiber

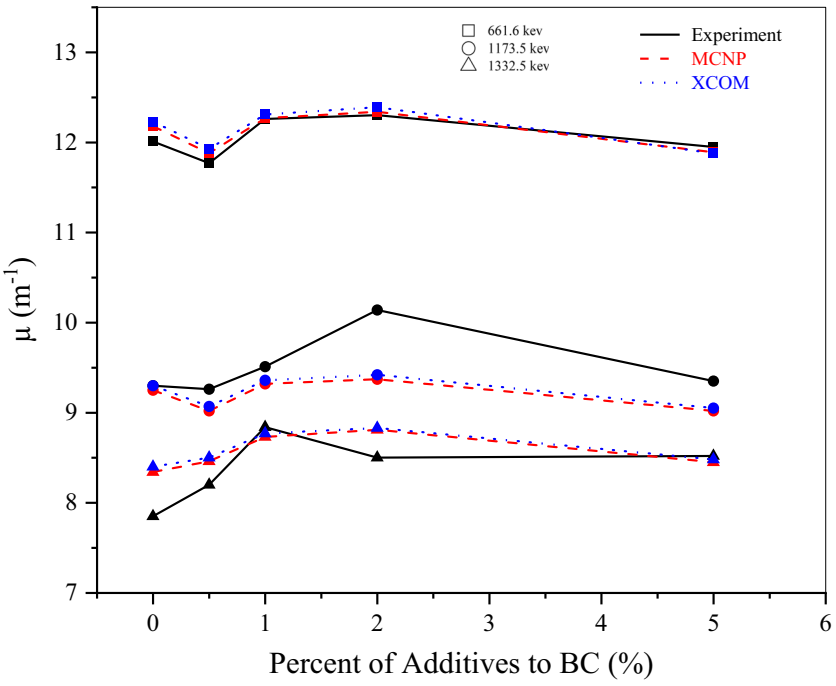

Fig. 10 The linear attenuation coefficient (μ) vs. the percentages of basalt fiber at three levels of energy

Table 6 HVL and TVL calculated based on theoretical formulae for the mixtures

Samples	Energy (keV)					
	661.6		1173.2		1332.5	
	TVL × 10^{-2} (m)	HVL × 10^{-2} (m)	TVL × 10^{-2} (m)	HVL × 10^{-2} (m)	TVL × 10^{-2} (m)	HVL × 10^{-2} (m)
BC	19.17	5.77	24.76	7.45	29.33	8.83
BCBF1	19.56	5.89	24.87	7.49	28.08	8.45
BCBF2	18.78	5.65	24.21	7.29	26.05	7.84
BCBF3	18.72	5.64	22.71	6.84	27.09	8.15
BCBF4	19.27	5.8	24.63	7.41	27.03	8.14

would decrease the thickness of the required thickness of the radiation shield layer.

As discussed, permeability is one of the key factors that should be controlled while modifying the clay soil barrier for radiation shielding applications. The permeability test results for the studied mixtures are presented in Figure 11. The graph clearly shows a relatively linear growth of the permeability coefficient by increasing the basalt fiber percentage. However, the rate of this increment varies between different basalt fiber percentages. This variation can be explained by the fact that by adding the fiber to the mixture first, an inhomogeneity is developed through the specimens, which slightly increases the hydraulic permeability (from BC to BCBF1), and then by adding more fiber, routs are created along the basalt fibers which facilitate the water permittivity through the mixture, and the connectivity of these routs significantly increases the hydraulic conductivity (from BCBF1 to BCBF2). After this stage, adding fibers only extends the created routs, which gradually increases the hydraulic permeability from BCBF3 to BCBF4.

Conclusions

In this research, the performance of the bentonite clay soil mixed with different percentages of basalt fibers as a radiation shielding barrier was investigated using experimental measurements, MCNP code, and XCOM web program. Good agreements were observed between the experimental and simulation results, where the maximum calculated propagation error value $\Delta(\mu)$ was 0.83 m^{-1}. Moreover, the hydraulic permeability, as a critical factor in landfill clay barriers, is controlled to be in the acceptable limit of the EPA standard. The hydraulic permeability grows by increasing the basalt fiber

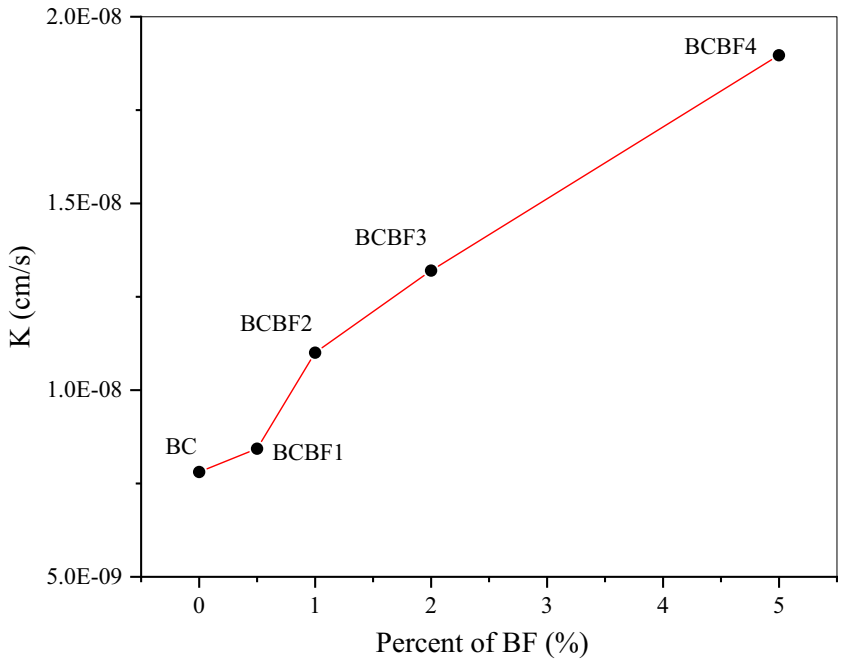

Fig. 11 The permeability test results for the studied mixtures

dosage. The maximum obtained permeability of 1.9×10^{-8} cm/s was for the BCBF4 sample, which is less than the maximum recommended value of 1×10^{-7} cm/s, by the EPA standard.

In general, the results indicated that the maximum linear attenuation coefficient is obtained for the 2% basalt fiber additive (BCBF3), 12.26, 9.51, and 8.84 m^{-1} at 661.6, 1173.2, and 1332.5 keV, respectively. As a result, the barrier thickness could be decreased using this mixture (BCBF3). To conclude, regarding the improved radiation shielding performance, workability, and acceptable hydraulic permeability, the mixture with 2% basalt fiber (BCBF3) could be an appropriate candidate to cover the radioactive waste disposal. For future researches, the use of basalt fiber as an additive in other materials such as concrete can be investigated for radiation shielding in other constructions such as nuclear power shields. Also, the epoxy resin is suggested to be used along with basalt fiber in the bentonite clay mixture to improve the continuity and homogeneity that may result in higher radiation attenuation and lower hydraulic permeability.

References

Akbulut S, Sehhatigdiri A, Eroglu H, Çelik S (2015) A research on the radiation shielding effects of clay, silica fume and cement samples. Radiat Phys Chem 117:88–92

Auerbach SI (1958) The soil ecosystem and radioactive waste disposal to the ground. Ecology 39(3):522–529

Barron EG, Dickman S (1949) Studies on the mechanism of action of ionizing radiations: II. Inhibition of sulfhydryl enzymes by alpha, beta, and gamma rays. J Gen Physiol 32(5):595–605

Briesmeister, J. F. (2000). MCNPTM-A general Monte Carlo N-particle transport code. Version 4C, LA-13709-M, Los Alamos National Laboratory, 2

Chilton AB, Shultis JK, Faw RE (1984) Principles of radiation shielding. Prentice-Hall, Englewood Cliffs

Day SR, O'Hannesin SF, Marsden L (1999) Geotechnical techniques for the construction of reactive barriers. J Hazard Mater 67(3):285–297

Divya PV, Viswanadham BVS, Gourc JP (2017a) Centrifuge modeling and digital image cross-correlation analysis of geofiber-reinforced clay-based landfill covers. J Geotech Geoenviron 143(1):04016076

Divya PV, Viswanadham BVS, Gourc JP (2017b) Centrifuge model study on the performance of fiber reinforced clay-based landfill covers subjected to flexural distress. Appl Clay Sci 142:173–184

Hejazi SM, Sheikhzadeh M, Abtahi SM, Zadhoush A (2012) A simple review of soil reinforcement by using natural and synthetic fibers. Constr Build Mater 30:100–116

Hicks TW, Baldwin TD, Hooker PJ, Richardson PJ, Chapman NA, McKinley IG, Neall FB (2008) Concepts for the geological disposal of intermediate-level radioactive waste. Sign 736:1

Hou Y, Li M, Gu Y, Yang Z, Li R, Zhang Z (2018) Gamma ray shielding property of tungsten powder modified continuous basalt fiber reinforced epoxy matrix composites. Polym Compos 39(S4):E2106–E2115

Hu H, Wang Q, Qin J, Wu Y, Zhang T, Xie Z, Zhang J et al (2008) Study on composite material for shielding mixed neutron and γ -rays. IEEE Trans Nucl Sci 55(4):2376–2384

Isfahani HS, Abtahi SM, Roshanzamir MA, Shirani A, Hejazi SM (2019a) Investigation on gamma-ray shielding and permeability of clay-steel slag mixture. Bull Eng Geol Environ 78(6):4589–4598

Isfahani HS, Abtahi SM, Roshanzamir MA, Shirani A, Hejazi SM (2019b) Permeability and gamma-ray shielding efficiency of clay modified by barite powder. Geotech Geol Eng 37(2):845–855

Jaeger, R. G., Blizard, E. P., Chilton, A. B., Grotenhuis, M., Hoenig, A., Jaeger, T. A., & Eisenlohr, H. H. (1968). Engineering compendium on radiation shielding volume I: shielding fundamentals and methods

Koch D (2002) Bentonites as a basic material for technical base liners and site encapsulation cut-off walls. Appl Clay Sci 21(1–2):1–11

Krane KS, Halliday D (1988) Introductory Nuclear Physics, section 9.6. Wiley, New York

Kroese DP, Brereton T, Taimre T, Botev ZI (2014) Why the Monte Carlo method is so important today. Wiley Interdisciplin Rev Comput Statist 6(6):386–392

Kucuk N, Tumsavas Z, Cakir M (2012) Determining photon energy absorption parameters for different soil samples. J Radiat Res 54(3):578–586

Li L, Lin C, Zhang Z (2017a) Utilization of shale-clay mixtures as a landfill liner material to retain heavy metals. Mater Des 114:73–82

Li R, Gu Y, Yang Z, Li M, Hou Y, Zhang Z (2017b) Gamma ray shielding property, shielding mechanism and predicting model of continuous basalt fiber reinforced polymer matrix composite containing functional filler. Mater Des 124:121–130

Li R, Gu Y, Zhang G, Yang Z, Li M, Zhang Z (2017c) Radiation shielding property of structural polymer composite: continuous basalt fiber reinforced epoxy matrix composite containing erbium oxide. Compos Sci Technol 143:67–74

Mahmoud KA, Tashlykov OL, Wakil AE, Zakaly HM, Aassy IE (2019) Investigation of radiation shielding properties for some building materials reinforced by basalt powder. In: AIP Conference Proceedings, vol 2174, No. 1. AIP Publishing LLC, Melville, p 020036

Mann HS, Brar GS, Mudahar GS (2016a) Gamma-ray shielding effectiveness of novel light-weight clay-flyash bricks. Radiat Phys Chem 127:97–101

Mann KS, Heer MS, Rani A (2016b) Investigation of clay bricks for storage facilities of radioactive-wastage. Appl Clay Sci 119:249–256

Martin JE (2006) Ch. 8: Radiation Shielding. In: Physics for radiation protection: a handbook. John Wiley & Sons, Hoboken, pp 367–423

Medjahed A, Derradji M, Zegaoui A, Wu R, Li B (2019) Mechanical and gamma rays shielding properties of a novel fiber-metal laminate based on a basalt/phthalonitrile composite and an Al-Li alloy. Compos Struct 210:421–429

Murphy MP, Hysong RJ, Edwards CW (1989) Low-level radioactive waste disposal technology development through a public process. Trans Am Nucl Soc 60

NIST XCOM. (2010). Element/compound/mixture - physical measurement, National Institude of Standard and Technology, **Retrieved from:** https://physics.nist.gov/PhysRefData/Xcom/Text/ref.html

Ono M, Shinsha H, Nakagawa D, Maruoka H, Tsutsumi A (2018) Work for volume reduction of clay in the new waste disposal area in Tokyo port. J JSCE 6(1):32–48

Prakash A, Poulose E (2016) Kuttanad clay amended laterite as a landfill liner for waste disposal facilities. Int J Scient Eng Res 4(3):75–78

Romanenko I, Holiuk M, Kutsyn P, Kutsyna I, Odynokin H, Nosovskyi A et al (2019) New composite material based on heavy concrete reinforced by basalt-boron fiber for radioactive waste management. EPJ Nuclear Sci Technol 5:22

Ryan M (1998) Planning and operation of low level waste disposal facilities. Health Phys 74:119

Seed, H. B., Wookward, R. J., & Lundgren, R. (1964). Clay mineralogical aspects of the Atterberg limits. Journal of Soil Mechanics & Foundations Div, 90(Proc. Paper 3983)

Shultis JK, Faw RE (2012) Radiation shielding. Encyclop Sustain Sci Technol:8536–8559

Skarżyński Ł (2020) Mechanical and radiation shielding properties of concrete reinforced with boron-basalt fibers using digital image correlation and X-ray micro-computed tomography. Constr Build Mater 255:119252

Weisstein, E. W. (2003). Eric Weisstein's world of physics. Retrieved from: http://scienceworld.wolfram.com/physics/MoessbauerSpectroscopy.html

Zegaoui A, Derradji M, Ghouti HA, Medjahed A, Zu LW, Liu WB et al (2019) Synergetic effects of short carbon/basalt hybrid fibers on the mechanical, thermal and nuclear shielding properties of DCBA/BA-a resin composites. Compo Commu 15:179–185

Zegaoui A, Derradji M, Medjahed A, Ghouti HA, Cai WA, Liu WB et al (2020) Exploring the hybrid effects of short glass/basalt fibers on the mechanical, thermal and gamma-radiation shielding properties of DCBA/BA-a resin composites. Polymer-Plastics Technol Mat 59(3):311–322

Zorla E, Ipbüker C, Biland A, Kiisk M, Kovaljov S, Tkaczyk AH, Gulik V (2017) Radiation shielding properties of high performance concrete reinforced with basalt fibers infused with natural and enriched boron. Nucl Eng Des 313:306–318